SBF
SOCIEDADE BRASILEIRA DE FÍSICA

NUCLEAR PHYSICS

Cluster Model Analysis of Pion Elastic and Inelastic Scattering from ^{12}C

Ahmed A. Ebrahim

Abstract Angular distributions of differential cross sections for the ^{12}C($\pi^\pm$, $\pi^\pm$)^{12}C and ^{12}C($\pi^\pm$, $\pi^\pm$)^{12}C* reactions at pion kinetic energy ranging from 50 to 260 MeV have been analyzed with the 3α-particle model of ^{12}C. The model provides good fits to a wide range of data. Differential cross sections for inelastic transitions to the (2^+; 4.44 MeV) and (3^-; 9.64 MeV) states in ^{12}C are computed and the deformation lengths δ_2 and δ_3 are extracted. It is found that the extracted deformation lengths are sensitive to the nuclear model used and similar to the corresponding values found with other probes and nuclear models.

Keywords Pion elastic scattering · Pion inelastic scattering · Distorted-wave Born approximation · Collective models · Cluster model

1 Introduction

Pion–nucleus scattering for energies from about 100–300 MeV can be described in terms of a simple optical potential which is of the form of the nuclear density multiplied by the elementary pion–nucleon off-shell T-matrix; the first-order pion–nucleus distorted-wave impulse approximation is used in the code DWPI [1]. The success of this first-order optical potential can be understood as a consequence of the dominance of the pion–nucleon (3,3) resonance in this energy region. Due to this resonance, the optical potential is highly absorptive

A. A. Ebrahim (✉)
Physics Department, Assiut University, Assiut 71516, Egypt
e-mail: a_ebrahim@yahoo.com

so that the mean free path of the pion is very small and consequently most of the scattering takes place in the nuclear surface. Possible second-order corrections to the optical potential necessarily involve the square of the density, so that they are strong only in the interior of the nucleus where the pion never gets the opportunity to enter [2, 3]. If one moves in energy away below the (3,3) resonance, the pion has more chance to sample the interior region of the nucleus and, consequently, higher-order effects could result [4, 5].

^{12}C is a nucleus which can be described in terms of an α-particle structure. It is considered to consist of three α-particles which basically retain the features of a free α-particle; each α-particle is bounded much more weakly than a nucleon in the ^{12}C nucleus. A local π-nucleus optical potential can be constructed based on the α-particle model of the ^{12}C nucleus, where the π-α amplitude can be directly obtained from the fitting of the experimental data.

Two forms of potential are commonly used to describe the pion–nucleus interaction. These are the Kisslinger [6] potential and a Laplacian [7] model. Both explicitly contain terms which originate in the p-wave pion–nucleon interaction, which requires, near the (3,3) resonance, a pion kinetic energy of about 165 MeV in the laboratory frame. The Kisslinger nonlocal potential [6] is

$$U_{\text{Kis}}(R) = \frac{(\hbar c)^2}{2\omega}\left\{q(R) + \nabla \cdot \alpha(R)\nabla\right\} \tag{1}$$

where ω is the total energy of the pion in the center of mass (c.m.) system, the quantities q and α(R) mainly result from the s- and p-waves of the pion–nucleon

interaction; they are complex and energy dependent [8].

Johnson and Satchler [8] used the Krell–Ericson transformation [9], which leads from the Klein–Gordon equation for pion scattering to a local potential for the transformed wave function, equivalent to Kisslinger nonlocal potential. This local potential was successfully used to analyze the elastic scattering from ^{12}C, ^{16}O, ^{28}Si, and ^{40,44,48}Ca in the pion kinetic energy range of 30 to 292 MeV [10, 11]. Empirical parameters, subject to a continuous ambiguity elastic and inelastic scattering of positive and negative pions from calcium isotopes and ^{54}Fe were studied using the Kisslinger local potential, together with a zero-range distorted-wave Born approximation (DWBA) code [12]. The local/zero-range DWBA code DWUCK4 [13] was used to calculate the differential cross section angular distributions for elastically and inelastically scattered pions from these targets. It was concluded that the DWUCK4 code and the local-equivalent Kisslinger potential of Johnson and Satchler are reliable models for pion–nucleus scattering.

The aim of the present work is to derive the optical potential for the reaction $\pi^{\pm}$-^{12}C when the nucleus is considered to be constructed of three alpha clusters. The derived optical potential is used to calculate the angular distributions of the differential cross sections of the $\pi^{\pm}$ elastically and inelastically scattered to the lowest 2^+ and 3^- states in ^{12}C in the energy range of 50–260 MeV.

2 Formalism

From the point of view of the nuclear cluster structure, ^{12}C is an example of a nucleus with an α-particle structure. In the following, we derive an analytical expressions of $\pi^{\pm}$-^{12}C potential with the 3α-cluster model of ^{12}C. The resulting potential is inserted into the DWUCK4 [13] code to calculate the differential cross sections for the reactions considered. The reactions are compared with the experimental data [14, 15].

The pion-α-particle potential is taken to be the nuclear local transformed potential [8]:

$$V_\alpha(R) = U_N(R) + \Delta U_C(R), \qquad (2)$$

where the Coulomb correction term $\Delta U_C(R)$ is [8]

$$\Delta U_C(R) = \frac{\alpha(R) V_C - (V_C^2/2\omega)}{1 - \alpha(R)}, \qquad (3)$$

and the nuclear local potential $U_N(R)$ is [8]

$$U_N(R) = \frac{(\hbar c)^2}{2\omega} \left\{ \frac{q(R)}{1 - \alpha(R)} - \frac{k^2 \alpha(R)}{1 - \alpha(R)} - \frac{\frac{1}{2}\nabla^2 \alpha(R)}{1 - \alpha(R)} \right. $$
$$\left. - \left(\frac{\frac{1}{2}\nabla\alpha(R)}{1 - \alpha(R)} \right)^2 \right\}. \qquad (4)$$

$q(R)$ and $\alpha(R)$ are similar to those in (1), they can be expressed in terms of the target nuclei density distributions and their gradients. $q(R)$ and $\alpha(R)$ are complex and energy dependent and given in detail in [8]. The pion–nucleon scattering amplitude depends on complex first- and second-order interaction parameters.

The first-order interaction parameters are related to the free pion–nucleon scattering through the phase shifts in the form described in [16–18], and the phase shifts are calculated according to the relation in [19]. The second-order parameters are required only at lower energies $T_\pi \leq 80$ MeV, but these parameters make no differences in the calculations at higher energies, so they were set to be zero [11, 19]. Here, V_C is the Coulomb potential due to the uniform charge distribution of the target nucleus of radius $R_C = r_C A^{1/3}$, where A is the target mass number and $r_C = 1.2$ fm [11].

The nuclear central optical potential of a pion incident on ^{12}C considered as 3α-clusters can be written in the form

$$V_{^{12}C}(R) = \int | \psi(\bar{r}, \bar{\rho}) |^2$$
$$\times \left[V_\alpha \left(\bar{R} + \frac{2}{3}\bar{\rho} \right) + V_\alpha \left(\bar{R} - \frac{1}{3}\bar{\rho} - \frac{1}{2}\bar{r} \right) \right.$$
$$\left. + V_\alpha \left(\bar{R} - \frac{1}{3}\bar{\rho} + \frac{1}{2}\bar{r} \right) \right] d\bar{r} \, d\bar{\rho}, \qquad (5)$$

where $\bar{R}$ is the separation vector between the centers of the two colliding particles. The internal position vectors $\bar{r}$ and $\bar{\rho}$ are defined by the position vectors of the three alpha particles $\bar{R}_1$, $\bar{R}_2$ and $\bar{R}_3$ constituting ^{12}C nucleus so that

$$\bar{r} = \bar{R}_2 - \bar{R}_1 \quad \text{and} \quad \bar{\rho} = \bar{R}_3 - \frac{1}{2}(\bar{R}_1 + \bar{R}_2),$$

The nuclear matter density distribution for an α-particle is

$$\rho_\alpha(r) = \rho_0 \, \exp(-\beta \, r^2), \qquad (6)$$

where $\rho_0 = 0.4229$ fm^{-3} and $\beta = 0.0.7014$ fm^{-2} [20].

The optical potential of each π-α particle in ^{12}C is given by V_α. The internal wave function of ^{12}C has the form [21]

$$\psi(\bar{r}, \bar{\rho}) = \left(\frac{2\sqrt{3}\,\mu}{\pi}\right)^{\frac{3}{2}} \exp\left(-\mu\left(2\,\rho^2 + \frac{3}{2}\,r^2\right)\right), \quad (7)$$

where μ is the range parameter of ^{12}C. We can decompose (5) into

$$V_{^{12}C}(R) = V_{\alpha 1}(R) + V_{\alpha 2}(R) + V_{\alpha 3}(R), \quad (8)$$

where

$$V_{\alpha 1}(R) = \int |\psi(\bar{r}, \bar{\rho})|^2 \left[V_\alpha\left(\bar{R} + \frac{2}{3}\,\bar{\rho}\right)\right] d\bar{r}\,d\bar{\rho},$$

$$V_{\alpha 2}(R) = \int |\psi(\bar{r}, \bar{\rho})|^2 \left[V_\alpha\left(\bar{R} - \frac{1}{3}\,\bar{\rho} - \frac{1}{2}\,\bar{r}\right)\right] d\bar{r}\,d\bar{\rho},$$

$$V_{\alpha 3}(R) = \int |\psi(\bar{r}, \bar{\rho})|^2 \left[V_\alpha\left(\bar{R} - \frac{1}{3}\,\bar{\rho} + \frac{1}{2}\,\bar{r}\right)\right] d\bar{r}\,d\bar{\rho}. \quad (9)$$

Since $\psi(\bar{r}, \bar{\rho})$ depends explicitly on the spatial coordinates $\bar{r}$ and $\bar{\rho}$ and $\psi(\bar{r}, \bar{\rho})$ is spatially symmetric about the exchange of nucleons [22], the integral is not changed if the Carbon coordinate system is reoriented each time so that the α cluster, which is being folded, lies along the vector $\bar{\rho}$. This allows the potential to be written as

$$V_{^{12}C}(R) = 3\,V_{\alpha 1}(R). \quad (10)$$

Using (2)–(7) and (10), we get for the $\pi^\pm$-^{12}C potential

$$\begin{aligned} V_{^{12}C}(R) \\ = 3 &\left[\frac{\rho_0\,\pi^3}{(s_{1i}\,s_{3i})^{\frac{3}{2}}}\left(\frac{2\sqrt{3}\,\mu}{\pi}\right)^3 \frac{\pi^3}{(y_i \cdot 3\,\mu)^{\frac{3}{2}}} \exp(-y_{2i}\,R^2)\right. \\ &\left. + \rho_0\left(\frac{\pi}{x_3}\right)^{\frac{3}{2}}\left(\frac{2\sqrt{3}\,\mu}{\pi}\right)^3 \frac{\pi^3}{(x_5 \cdot 3\,\mu)^{\frac{3}{2}}} \exp(-x_6\,R^2)\right], \end{aligned}$$
$$(11)$$

where

$$y_i = 4\,\mu + \frac{4}{9}\,s_{4i}, \quad (12)$$

$$y_{2i} = s_{4i} - \frac{4\,(s_{4i})^2}{9\,y_i}, \quad (13)$$

$$x_5 = 4\,\mu + \frac{4}{9}\,x_4, \quad (14)$$

$$x_6 = x_4 - \frac{4\,(x_4)^2}{9\,x_5}, \quad (15)$$

while

$$s_{1i} = \beta + q(R), \quad (16)$$

$$s_{2i} = q(R) - \frac{(q(R))^2}{s_{1i}}, \quad (17)$$

$$s_{3i} = \alpha(R) + s_{2i}, \quad (18)$$

$$s_{4i} = s_{2i} - \frac{s_{2i}^2}{s_{3i}}, \quad (19)$$

and

$$x_3 = \beta + \alpha(R), \quad (20)$$

$$x_4 = \alpha(R) - \frac{(\alpha(R))^2}{x_3}. \quad (21)$$

The radial parts of the hadronic inelastic transition potential used here are

$$F_l(R) = -\gamma_l^N \frac{dU_{^{12}C}(R)}{dR}, \quad (22)$$

where $U_{^{12}C}(R)$ is the optical potential found to fit the corresponding elastic scattering (11). For a given transition, we use γ_l^N with $N = \pm$ to denote the corresponding deformation lengths for the $\pi^\pm$ interaction, while $l(= 2$ or $3)$ is the multipolarity; γ_2 denotes the corresponding deformation length for the transition to the $(2^+; 4.44$ MeV$)$ and γ_3 to the transition to the $(3^-; 9.64$ MeV$)$ states in ^{12}C.

3 Results and Discussion

The DWBA calculations were performed using the computer code DWUCK4 [13]. The radial integrals have been carried out up to 20 fm with 0.05 steps and 100 partial waves. The Coulomb potential was obtained using a charge distribution of the target nucleus of radius R_C [11].

We analyzed the angular distribution of differential cross sections for the elastic and inelastic scattering of $\pi^\pm$ from ^{12}C in the pion kinetic energy range of 50 to 260 MeV. The central optical potential used here (9) is integrated and inserted into the DWUCK4 program. The complex local optical potential V_α is calculated using the expressions from [10].

The resulting kinematic and parameter values for the cases studied here are calculated according to equations given in [10] and are listed in Table 1. For elastic and inelastic scattering from ^{12}C, the values of the first- and second-order parameters are the same for both beam charges. In the present calculations we used the Ericson–Ericson Lorentz–Lorentz parameter $\zeta = 1.0$; this is more suitable for $\pi^\pm$-nucleus scattering using the

Table 1 Kinematic factors for use in a nonrelativistic Schrödinger equation used in the present work with pion kinetic energy T_π. E_L, M_π, k and p_1 are the effective bombarding energy, effective pion mass, pion wave number, and kinematic transformation factor, respectively

T_π (MeV)	E_L (MeV)	M_π (u)	k (fm^{-1})	p_1
50	43.63	0.20189	0.639	1.1825
150	113.30	0.30501	1.254	1.2726
180	132.20	0.33558	1.417	1.2992
220	156.32	0.37543	1.625	1.3345
260	180.66	0.41629	1.833	1.3687

Kisslinger local potential in the energy range considered here [11].

The present optical potential of ^{12}C predicts well the maximum and minimum positions with those calculated in [23] for the elastic and inelastic scattering differential cross sections at large angles according to the choice of the wave function with $\mu = 0.04667$ fm^{-2}. This agrees well with the reported results for the α-particle model

of ^{12}C-^{12}C reaction [24]. In particular, our calculations predict two diffraction minima at 150 and 180 MeV, but the predicted minima are much deeper than those observed.

In Fig. 1, the measured elastic scattering differential cross sections at forward angles and the positions of the minima and the maxima agree well with our calculations at the three energies 150, 180, and 260 MeV ($\chi^2 = 3.20$–5.12). The short mean free path of the pion in the Δ-region produces pronounced Fraunhofer diffraction patterns in the elastic scattering from nuclei; this appears clearly in Fig. 1. Outside the resonance region the diffractive character of the angular distributions is still apparent, but less pronounced. In particular, the minima are systematically more shallow both above and below the resonance.

The present π^--^{12}C optical potential is shown in Fig. 2 at 190 MeV. From that figure it is seen that in this case the real (imaginary) part is quite shallow and everywhere attractive (absorptive). The imaginary part is deeper and rapidly decreasing while the real part is shallower and wider.
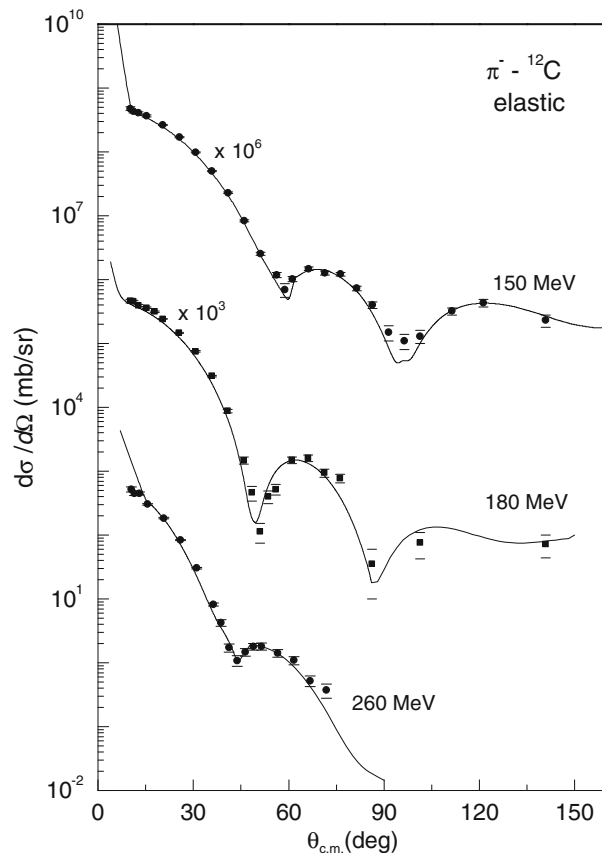

Fig. 1 Elastic scattering differential cross sections for 150, 180 and 260 MeV π^- on ^{12}C. *Solid curves* represent our potential model calculations. *Solid points* represent the experimental data taken from [14]
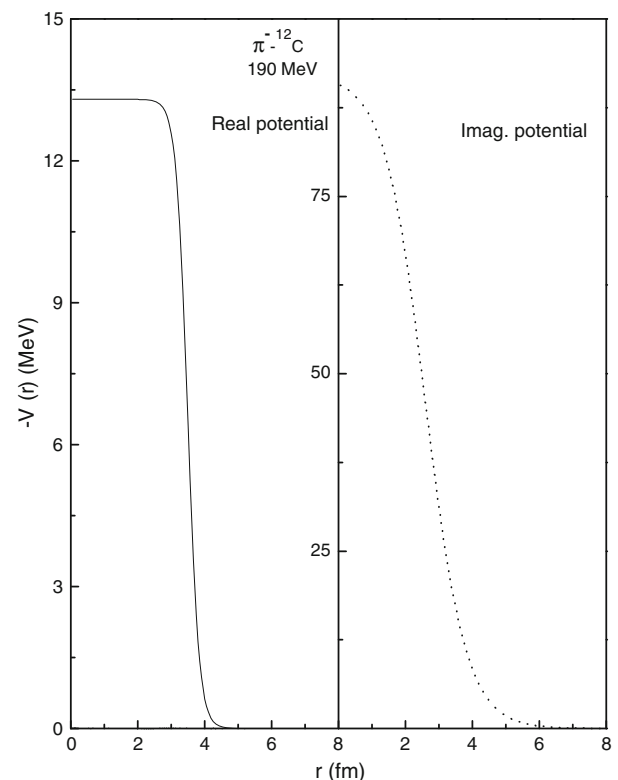

Fig. 2 The optical potentials computed for 190 MeV π^- scattered from 3α-cluster of ^{12}C. The *solid curve* represents the real potential, and the *dotted curve* represents the imaginary potential

In Fig. 3, at lower pion beam energies <100 MeV, the second-order parameters are necessary to explain the data. The elastic scattering differential cross sections of $\pi^\pm$ from ^{12}C at the pion kinetic energy 50 MeV are calculated using the present potential model. The present optical potential calculations are in good agreement with the experimental data when the second-order parameters are included in addition to the first-order parameters with $\chi^2 = 3.5$ for π^+ and 2.24 for π^-.

As $k \longrightarrow 0$, the s-wave scattering length is $a_0 = \delta_0/k$ and p-wave scattering volume is $a_1 = \delta_1/k^3$, where δ_0 and δ_1 are respectively the s- and p-wave phase shifts. Here a_0 and a_1 are calculated at 1 keV for pions of both signs with the Coulomb potential omitted for the present optical potential [25]. The magnitude of a is a measure of the strength of the interaction and its sign indicates whether the interaction is effectively repulsive or attractive. The scattering lengths and volumes calculated from our potential model are listed in Table 2 along with the values obtained from [25, 26]. The values

Table 2 Zero-energy pion-^{12}C s-wave scattering lengths a_0 (fm) and p-wave scattering volumes a_1 (fm^3) calculated using the present optical potential compared with other works

	Present cals.	Others [25, 26]
Rea_0	−0.445	−0.438 $\longrightarrow$ −0.449
Ima_0	0.127	0.122 $\longrightarrow$ 0.129
Rea_1	1.85	1.88 $\longrightarrow$ 1.93
Ima_1	0.494	0.347 $\longrightarrow$ 0.553

of a_0 and a_1 calculated here are in a good agreement in sign and magnitude with those of [25, 26].

Since inelastic scattering in the collective model is driven by the first derivative of the optical potential, agreement with such data can be a possible tool to remove the ambiguity from elastic scattering fits using the local potential [27]. Here, angular distributions for the inelastic scattering of pions leading to the lowest 2^+ and 3^- states in ^{12}C are computed by the DWBA method using the zero-range code DWUCK4 [13]. The α-particle model optical potential may be tested, to
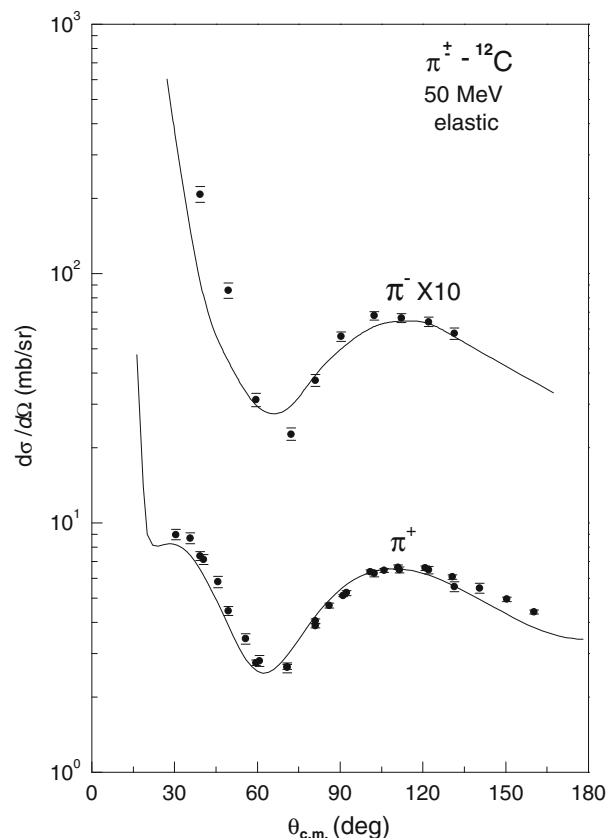

Fig. 3 As in Fig. 1, but for $\pi^\pm$–^{12}C elastic scattering differential cross sections at 50 MeV pion kinetic energy. The experimental data are taken from [15]
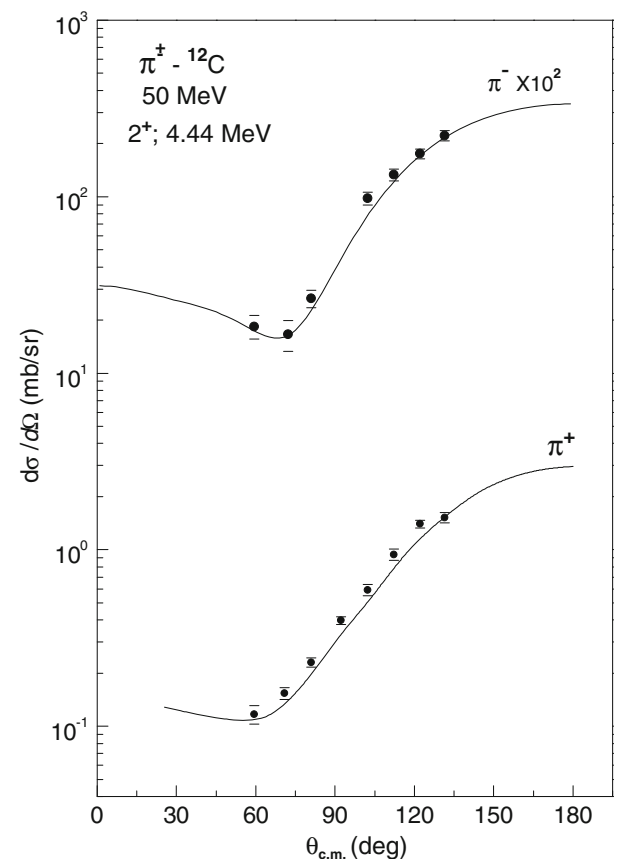

Fig. 4 As in Fig. 3, but for inelastic scattering differential cross sections of 50 MeV $\pi^\pm$ exciting the 4.44 MeV 2^+ state of ^{12}C. The experimental data are taken from [15]

predict observables of $\pi^{\pm}$ inelastically scattered from nuclei. A collective model DWBA prediction using our potential model adequately fits the shape and magnitude of 50–260 MeV pion kinetic energies leading to the lowest 2^+ and 3^- states in ^{12}C as shown in Figs. 4, 5 and 6. In the analysis presented here, the deformation lengths are varied until agreement is obtained with $\pi^{\pm}$ data.

Figure 4 displays the predictions of the inelastic scattering differential cross sections of $\pi^{\pm}$ from ^{12}C nucleus excited to the lowest 2^+ state at 50 MeV. The inelastic data [15] are well represented by our calculations with $\chi^2 = 1.73$ for π^+ and 2.15 for π^-, when the first and second-order parameters are included in our potential model.

Figures 5 and 6 display the predictions of the inelastic scattering differential cross sections of π^- from ^{12}C excited to the lowest 2^+ and 3^- states at 150, 180, and 260 MeV. Our local potential predictions seem to be in better agreement with inelastic scattering data [14]
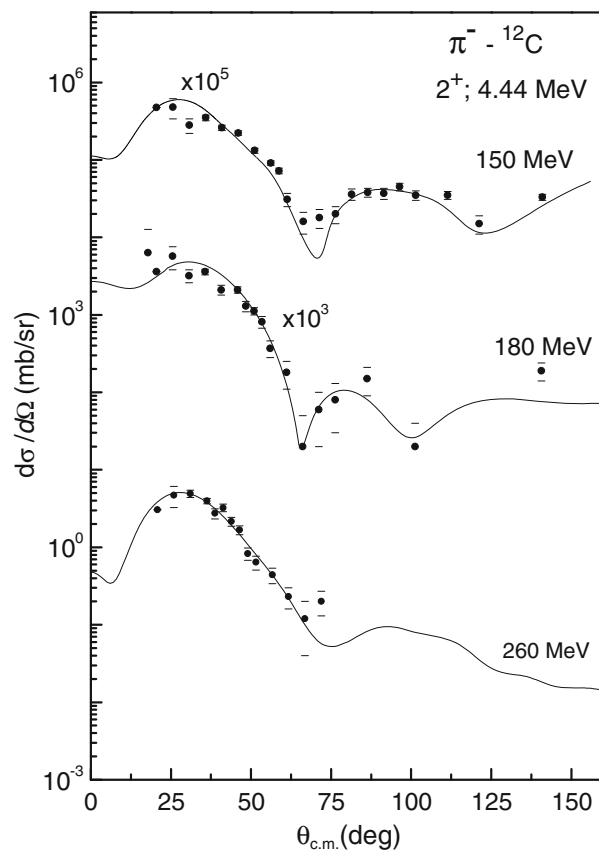

Fig. 6 As in Fig. 5 but for the 9.64 MeV 3^- state of ^{12}C

Fig. 5 As in Fig. 4 but for inelastic scattering differential cross sections of 150, 180, and 260 MeV π^- exciting the 4.44 MeV 2^+ state of ^{12}C. The experimental data are taken from [14]
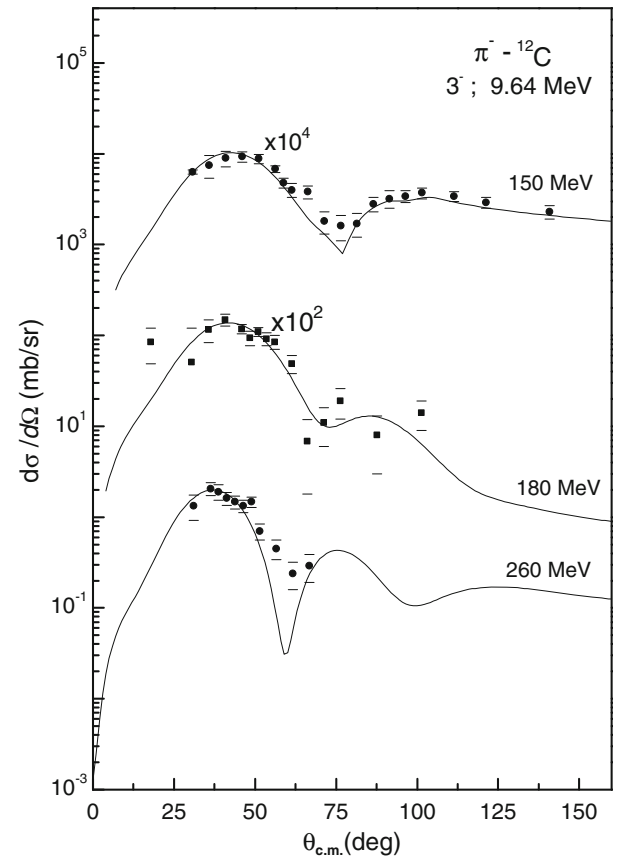
at all energies considered in the present work with χ^2 ranging from 3.5 to 5.29 for 2^+ and 1.7 to 3.49 for 3^- states.

From the above, we note that the fits reproduced on the basis of the α-cluster model of ^{12}C nucleus are more reasonable for low-energy pions than for pions of higher energies. This may indicate that the clustering phenomena in ^{12}C nucleus is more dominant for low pion energy scattering while pions of higher energies prefer to interact with ^{12}C nucleus as a whole. The predictions of our potential well fit the data for differential cross sections at all energies under consideration.

The resulting deformation lengths for all collective states from the present potential model, determined by visually adjusting the calculations to reproduce the data are listed in Table 3 compared with those obtained from the corresponding ones previously extracted by others [28–31]. It is clear from Table 3 that the deformation lengths of the real potential are greater than the corresponding ones for the imaginary potential in all cases under consideration. Real deformation lengths

Table 3 Deformation lengths from $\pi^{\pm}$ inelastic scattering on ^{12}C calculated using the present potential model compared with those extracted from other particles on ^{12}C [28–31]

State	2^+					3^-		
Pion	π^+	π^-				π^-		
T_π (MeV)	50	50	150	180	260	150	180	260
The present model								
γ_{real} (fm)	1.514	1.406	1.325	1.452	1.536	1.266	1.182	1.335
γ_{imag} (fm)	1.208	1.117	1.195	1.215	1.307	1.007	0.812	1.214
χ^2	1.730	2.150	3.520	4.780	5.290	1.730	3.250	3.490
Others								
γ (fm)	1.12–1.97	1.02–1.41	1.07 ± 0.05	1.50–1.21	0.65–1.23			
References	[28]	[29]	[30]	[31]	[28]			
Reaction	p-^{12}C	^{3}He-^{12}C	α-^{12}C	^{16}O-^{12}C	^{12}C-^{12}C			
	d-^{12}C				α-^{12}C			
	^{3}He-^{12}C					^{16}O-^{12}C		

The corresponding χ^2 values are also calculated

extracted here at 150 MeV for 2^+ and 180 MeV for 3^- are minimum. All values of the deformation lengths extracted from the present work lie within or very close to the range of the corresponding values previously extracted from other particles on ^{12}C [28–31]. It can be seen from Table 3 that the values of imaginary deformation lengths determined here using the present potential model for the 2^+ and 3^- excited states in ^{12}C increase with increasing pion kinetic energy, except for the case of 180 MeV π^- inelastic scattering off 3^- state in ^{12}C. This 180 MeV energy lies in the (3,3) resonance region of pions. Table 3 also includes the calculated χ^2 values corresponding to each case under consideration. Again, it shows that χ^2 is minimum for our potential model at each of these cases except for π^- inelastic scattering of 150 MeV kinetic energy scattered to 2^+ and 3^- excited states in ^{12}C.

The DWUCK4 code along with our potential model calculates the reaction cross sections σ_R of pion scattering from ^{12}C at pion kinetic energy ranging from 50 to 260 MeV. Following the same procedure the total cross sections σ_T are calculated using the reported formula in [32]. Table 4 shows the predicted σ_R and σ_T for pions of both signs scattering on ^{12}C at 50–260 MeV pion kinetic energy together with the corresponding cross sections estimated by others [14, 23, 25, 33]. The values of σ_R and σ_T predicted by the present potential model are very close to the corresponding cross sections estimated by others. This result is not surprising in view of the short mean free path of pions in nuclei in this energy range which should make most of the scattering take place in the nuclear surface. This is in contrast with the situation of low-energy pions [33].

From Table 4, it is noticed for $\pi^{\pm}$ scattering of $T_\pi \geq$ 180 MeV from ^{12}C that both calculated σ_T and σ_R decrease as the beam energy increases. At all considered energies, values of σ_T for π^- are greater than those for π^+ at a certain energy. This indicates that the mean free path λ for π^- is shorter than the corresponding λ for π^+. This is consistent with our previous results [12].

Table 4 Total and reaction cross sections in mb for $\pi^{\pm}$ scattering on ^{12}C calculated in the present work compared with other works

T_π (MeV)	Pion	Present cals.		Others		
		σ_T	σ_R	σ_T	σ_R	References
50	π^+	265.35	159.80	228.0	160.0	[25]
				248 ± 20	152 ± 14	[33]
180		575.5	376.2	581.0	384.0	[25]
220		525.4	319.7	521.0	318.0	[25]
50	π^-	295.8	195.6	290.0	200.0	[25]
150		685.4	435.8	696 ± 7		[14]
180		650.6	414.6	615.0	400.0	[25]
				670 ± 7		[14]
220		570.4	336.9	552.0	330.0	[25]
				586.0		[23]
260		540.4	324.3	536 ± 6		[14]

4 Conclusions

Elastic, inelastic, total, and reaction cross sections have been calculated, using DWBA with zero-range DWUCK4 code using our potential, which is based on the 3α-particle model formalisms for π-nucleus reactions. We have been able to obtain a good fit to the data for the elastic and inelastic scattering of 50–260 MeV pions from ^{12}C. The V_α used in our potential model emphasizes a careful treatment of the first and second-order optical potential. This potential includes also short-range correlations ζ.

The deformation lengths and parameters determined from the present analysis are in agreement with the deformations determined using other probes. This collective model analysis is successful in its description of the reaction dynamics and the structure of the collective, $N = Z$ nucleus.

Given its success, the analysis of pions scattered from ^{12}C, based on the 3α-cluster model, with the DWUCK4 program, is being extended to compute the differential elastic and inelastic cross sections and coupled channels reactions for pions from other nuclei.

References

1. R.A. Eisenstein, G.A. Miller, Comput. Phys. Commun. **11**, 95 (1976)
2. E. Friedman, et al., Phys. Rev. C **72**, 034609 (2005)
3. M. Döring, E. Oset, Phys. Rev. C **77**, 024602 (2008)
4. M.B. Johnson, Phys. Rev. C **22**, 192 (1980)
5. M.B. Johnson, E.R. Siciliano, Phys. Rev. C **27**, 1647 (1983)
6. L.S. Kisslinger, Phys. Rev. **98**, 761 (1955)
7. G. Fäldt, Phys. Rev. C **5**, 400 (1972)
8. M.B. Johnson, G.R. Satchler, Ann. Phys. N.Y. **248**, 134 (1996)
9. M. Krell, T.E.O. Ericson, Nucl. Phys. B **11**, 521 (1969)
10. G.R. Satchler, Nucl. Phys. A **540**, 533 (1992)
11. S.A.E. Khallaf, A.A. Ebrahim, Phys. Rev. C **62**, 024603 (2000)
12. S.A.E. Khallaf, A.A. Ebrahim, Phys. Rev. C **65**, 064605 (2002)
13. P.D. Kunz, DWUCK4 Computer Code, University of Colorado (unpublished)
14. F. Binon, P. Duteil, J.P. Garron, J. Gorres, L. Hugon, J.P. Peigneux, C. Schmit, M. Spighel, J.P. Stroot, Nucl. Phys. B **17**, 168 (1970)
15. R.J. Sobie, et al., Phys. Rev. C **30**, 1612 (1984)
16. J. Bartel, M.B. Johnson, M.K. Singham, Ann. Phys. (N.Y.) **196**, 89 (1989)
17. S.J. Greene, et al., Phys. Rev. C **30**, 2003 (1984)
18. R.A. Gilman, Ph.D. dissertation, University of Pennsylvania (1985)
19. S.A.E. Khallaf, A.A. Ebrahim, Phys. Rev. C **54**, 2499 (1996)
20. G.R. Satchler, W.G. Love, Phys. Rep. **55**, 193 (1979)
21. M.W. Kermode, Proc. Phys. Soc. **84**, 554 (1964)
22. S.A.E. Khallaf, M. El-Azab, Atomkernenergie/Kerntechnik **37**, 294 (1981)
23. L. Qing-Run, Nucl. Phys. A **415**, 445 (1984)
24. S.A.E. Khallaf, M. Abdelrahman, S. Abdelraheem, S. Mahmoud, Jpn. J. Appl. Phys. **37**, 657 (1988)
25. K. Stricker, H. McManus, J.A. Carr, Phys. Rev. C **19**, 929 (1979)
26. J. Hüfner, Phys. Rep. **21**C, 1 (1975)
27. Md.A.E. Akhter, S.A. Sultana, H.M. sen Gupta, R.J. Peterson, J. Phys. G **27**, 755 (2001)
28. S.M. Smith, G. Tibell, A.A. Cowley, D.A. Goldberg, H.G. Pugh, W. Reichart, N.S. Wall, Nucl. Phys. A **207**, 273 (1973) and references therein
29. A.S. Dem' yanova, E.F. Svinareva, S.A. Goncharov, S.N. Ershov, F.A. Gareev, G.S. Kazacha, A.A. Ogloblin, J.S. Vaagen, Nucl. Phys. A **542**, 208 (1992)
30. M.E. Brandan, K.W. McVoy, Phys. Rev. C **43**, 1140 (1991)
31. P.J. Moffa, C.B. Dover, J.P. Vary, Phys. Rev. C **16**, 1857 (1977)
32. A.A. Ebrahim, S.A.E. Khallaf, Phys. Rev. C **66**, 044614 (2002)
33. A. Saunders, S. Høibråten, J.J. Kraushaar, B.J. Kriss, R.J. Peterson, R.A. Ristinen, J.T. Brack, G. Hofman, E.F. Gibson, C.L. Morris, Phys. Rev. C **53**, 1745 (1996)